Stochastic model of lithium ion conduction in poly(ethylene oxide)

L. Gitelman,[1] A. Averbuch,[2,a)] M. Nathan,[3] Z. Schuss,[4] and D. Golodnitsky[5]
[1]*Faculty of Applied Mathematics, Technion, Haifa 32000, Israel*
[2]*School of Computer Science, Tel Aviv University, Tel Aviv 69978, Israel*
[3]*School of Electrical Engineering, Tel Aviv University, Tel Aviv 69978, Israel*
[4]*Department of Mathematics, Tel Aviv University, Tel Aviv 69978, Israel*
[5]*School of Chemistry, Tel Aviv University, Tel Aviv 69978, Israel*

(Received 19 October 2009; accepted 4 February 2010; published online 30 March 2010)

We develop, analyze, and simulate a physical model of Li^+-ion conduction inside polyethylene oxide (PEO) helical tubes, which are the solvent of LiI salt. The current is due to diffusion and electric interactions with a permanent external field, the PEO charges, and ion-ion interactions. Potential barriers are created in the PEO by loops in structure. We calculate the energy of configurations of one or two lithium ions in the loop and derive an explicit expression for the activation energy. We use Kramers' formula to calculate the conductivity as function of mechanical stretching, which lowers the barrier and causes an exponential rise in the output conductivity.
 [doi:10.1063/1.3357272]

I. INTRODUCTION

In Refs. 1 and 2, we developed a model of lithium ion conduction in dilute and concentrated polymer electrolytes $(LiI:P(EO)_n(3 \le n \le 100))$, based on an analogy between protein channels of biological membranes that conduct Na^+, K^+, and other ions,[3–6] and the polyethylene oxide (PEO) helical chain that conducts Li^+ ions. There are, however, significant differences between them, while protein channels are embedded in the cell membrane and their nearly rectilinear pores are aligned, the PEO molecules contain loops and their directions are random (see Fig. 1). When a voltage drop exists between the terminals of the loop, ions have to diffuse up potential gradients in order to traverse the loop and reach the cathode. Diffusion over potential barriers gives rise to an Arrhenius-type relation between voltage and current.[11] Unfolding the loops by mechanical stretching can, therefore, affect the conductivity of a PEO electrolyte in a decisive fashion. While[2] presents simulations of PEO loops with various degrees of stretching, our purpose in this paper is to elucidate, both analytically and numerically, the effect of stretching and concentration on PEO conductivity.

To make this paper self-contained, we recall some basic facts from Ref. 2. In our model the PEO chains adopt a helical conformation with all C–O bonds trans and C–C bonds either gauche or gauche minus.[5] We assume that there are no ionic cross-links between chains and there are only weak van der Waals interactions. Typically, the composition of polymer-salt complex is 3:1. Changing the polymer-salt ratio from 3:1 to 1:1 has a profound influence on the PE structure.[5] The polymer chain conformation changes from helical to a stretched zigzag arrangement and the cations are coordinated by only two ether oxygens and four anions. The anions coordinate simultaneously cations, which are themselves associated with different PEO chains. As a result, there is extensive interchain cross-linking in the 1:1 complexes.

Increasing the polymer-salt ratio from 3:1 to 6:1 has an equally profound influence on the crystal structure (see Ref. 5). The cations are arranged in rows, where each row is located within a cylindrical tunnel formed by two PEO chains. Each chain forms the surface of a half-cylinder and the two chains interlock on each side to complete the cylindrical arrangement. The anions do not coordinate the cations, but are instead located outside the PEO cylinder in the interchain space. The anions are also arranged in rows.

On passing from the crystalline to the amorphous state, the structure is largely retained with only a loss of register between the chains, leading to disruption of the long range order.[5] In particular, it appears that the PEO chain retains its helical conformation while the cations remain inside the helices and are associated with their anions. The fact that in both 3:1 and 6:1 compositions the cations remain within tunnels defined by the PEO chains suggests that cation transport occurs preferentially along such tunnels, with the rate limiting step being transfer between tunnels, in agreement with Ref. 4.

II. THE PHYSICAL MODEL

We assume that the as-cast PEO under consideration consists of long helical chains of small radius, whose axes are oriented randomly. The axis of each chain is bent many times, forming a random helix. We consider one turn of such a helix and assume it is a circular loop (see Fig. 2). The equation of the helical loop is

$$\boldsymbol{x}=\begin{pmatrix} R\cos\left(t-\frac{\pi}{2}\right) \\ R\sin\left(t-\frac{\pi}{2}\right) \\ \frac{dt}{2\pi} \end{pmatrix}, \quad 0<t<2\pi, \tag{1}$$

a)Electronic mail: amir@math.tau.ac.il.

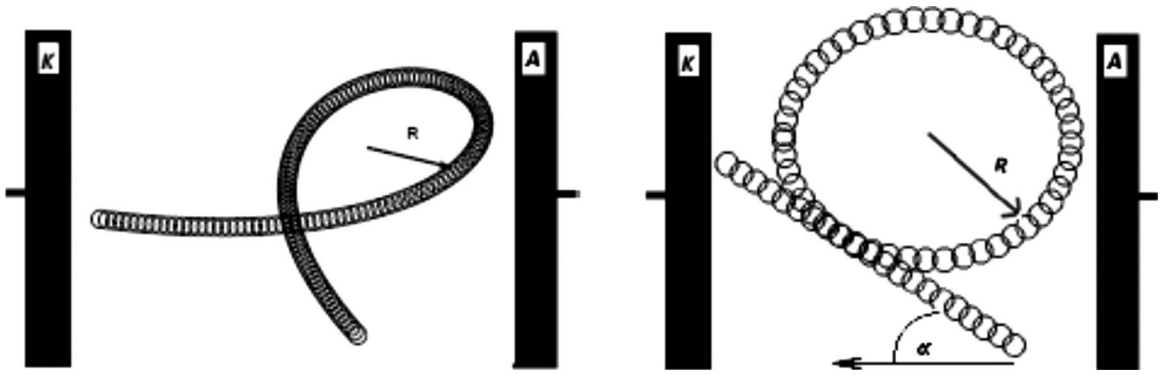

FIG. 1. Left panel: the helical loop and right panel: closeup of the loop.

where d is the step of the helix.

The random loop radius is assumed to be significantly longer than the random step of a helical turn. The axis of the random helix, which is essentially a bundle of loops, is inclined relative to the line perpendicular to the electrodes A and K, which are a distance $L \approx 100$ μm apart and the voltage drop between them is $\Delta V = 3-3.5$ V, depending on the cathode materials used in a lithium/polymer electrolyte battery (see 1 for a single chain that bridges the gap). The dielectric constant of the PEO is $\varepsilon = 2.5$. The angle of inclination α is assumed uniformly distributed in the interval $0 \leq \alpha \leq \pi/2$. For $\alpha = 0$, the main lithium ion transport mechanism is diffusion and transport down the potential gradient inside the channel.

A. The structure of the PEO

The solenoidal PEO helix, Fig. 3, is replaced (Refs. 7 and 10) with a sequence of 2294 units of CH_2-CH_2-O, seven units of CH_2-CH_2-O per two turns of the narrow helix (see Fig. 3). The length of two turns of the narrow helix is $d = 1.93$ nm. The units of CH_2 are at a distance $r_{CH} = 0.1$ nm from the x-axis, which is the axis of a linear segment of the narrow helix, and the units of O are at a distance $r_O = 0.04$ nm from the x-axis. Typical charge distribution values are +0.245 for a unit of CH_2 and -0.406 for a unit of O.[8–10]

The spatial structure of the PEO is that of a random helix formed by the narrow helix—see Fig. 1. We measure arclength s along the axis of the narrow helix and use it as a global coordinate of a lithium ion.

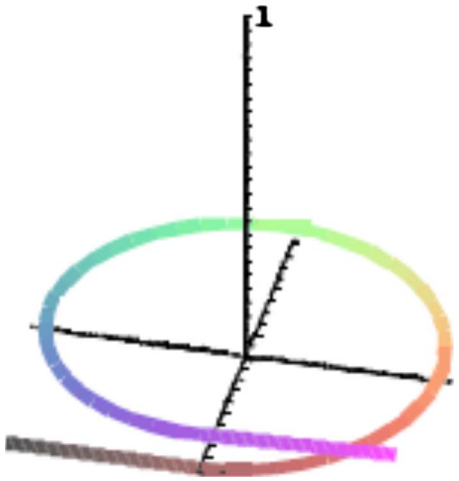

FIG. 2. (Color online) The polymer folded into a helix containing a circular loop.

B. The electric potential

We consider only the effect of the loop on the conductivity of the PEO and disregard the Coulombic potential of the permanent charges in the polymer. To show that this is a valid approximation, we write the potential created in a loop of radius R in a plane perpendicular to the electrodes at arclength s on the axis of the narrow helix by the PEO charges as[2]

$$\Phi(s) = \frac{1}{4\pi\varepsilon_0\varepsilon}\sum_{j=1}^{N}\left[\sum_{i=1}^{n_1}\frac{q^+}{\sqrt{4R^2\sin^2\left(\frac{s-s_{ij}^+}{2R}\right)+r_{CH}^2}} + \sum_{i=1}^{n_2}\frac{q^-}{\sqrt{4R^2\sin^2\left(\frac{s-s_{ij}^-}{2R}\right)+r_O^2}}\right], \quad (2)$$

where q^- and q^+ are the net negative and positive charges on a ring, s_{ij}^+ and s_{ij}^- are, respectively, the coordinates of the units CH_2 and O, and n_1 and n_2 are the numbers of positive and negative particles in the loop, respectively. The potential of the field created by an applied external voltage in a direction perpendicular to the plane of the electrodes is

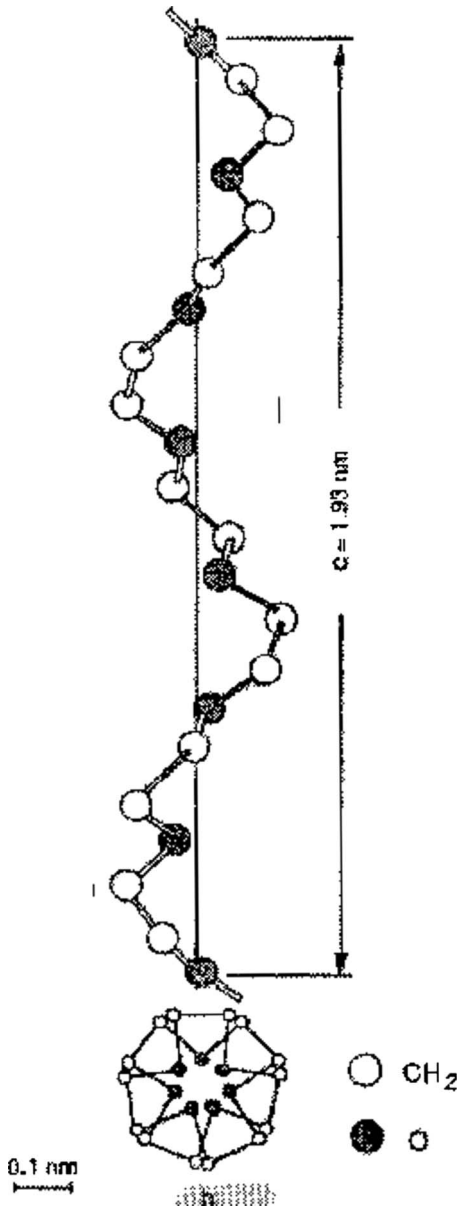

FIG. 3. Schematic model of poly(ethylene oxide). The same two turns of the helix appear at the bottom of the figure.

$$\Psi_E(s) = -\frac{V_K - V_A}{\varepsilon L} x \sin\ \eta = -ER\cos\left(\frac{s}{R}\right)\sin\ \eta,$$

where $E = V_K - V_A/\varepsilon L$ and η is the angle between the plane of the loop and the plane of the electrodes. We write the configuration space coordinates of the lithium and iodide ions, respectively, as

$$\boldsymbol{s} = (s_1, s_2, \ldots, s_L), \quad \boldsymbol{s}' = (s_1', s_2', \ldots, s_L').$$

The potential of the electric field acting on the nth lithium ion at s_n in the loop, including the Coulombic potential of the interionic forces is

$$\Psi_{\mathrm{Li}^+}(\boldsymbol{s},\boldsymbol{s}') = \frac{1}{4\pi\varepsilon_0\varepsilon}\sum_{i\neq n}\frac{q_{\mathrm{Li}^+}}{2R\left|\sin\left(\frac{s_n - s_i}{2R}\right)\right|} + \frac{1}{4\pi\varepsilon_0\varepsilon}\sum_{i=1}^{L}\frac{q_{I^-}}{\sqrt{4R^2\sin^2\left(\frac{s_n - s_i'}{2R}\right) + r_{\mathrm{CH}}^2}} + \Phi(s_n) + \Psi_E(s_n),$$

and that of the force acting on the nth iodide ion at s_n' is

$$\Psi_{I^-}(\boldsymbol{s},\boldsymbol{s}') = \frac{1}{4\pi\varepsilon_0\varepsilon}\sum_{i=1}^{L}\frac{q_{\mathrm{Li}^+}}{\sqrt{4R^2\sin^2\left(\frac{s_n' - s_i}{2R}\right) + r_{\mathrm{CH}}^2}} + \frac{1}{4\pi\varepsilon_0\varepsilon}\sum_{i\neq n}\frac{q_{I^-}}{2R\left|\sin\left(\frac{s_n' - s_i'}{2R}\right)\right|} + \Phi(s_n') + \Psi_E(s_n').$$

A more complex configuration consists of N linear segments of lengths S_i, inclined at angles $0 \le \alpha_i \le \pi/2$, $(i = 1,2,\ldots,N)$, and $N-1$ circular loops of radii R_i, attached at the ends of the linear segments at angles $0 \le \eta_i \le \pi/2$, $(i = 1,2,\ldots,N-1)$, respectively. The end points of the linear segments are the arclengths

$$\lambda_k = \sum_{i=1}^{k-1} S_i + 2\pi\sum_{i=1}^{k-1} R_i, \quad \mu_k = \sum_{i=1}^{k} S_i + 2\pi\sum_{i=1}^{k-1} R_i, \quad (k = 1,2\ldots,N),$$

and the arclengths in the loops are $\mu_k \le s \le \lambda_{k+1}$, $(k = 1,2,\ldots,N-1)$. Note that $\lambda_1 = 0$ and $\Psi_E(\lambda_1) = V_A$, and $\Psi_E(\lambda_{k+1}) = \Psi_E(\mu_k)$. The electric potential of the applied voltage is

$$\Psi_E(s) = \begin{cases} -E(s-\lambda_k)\cos\ \alpha_k + \Psi_E(\lambda_k) & \text{if } \lambda_k \le s \le \mu_k,\ k = 1,\ldots,N \\ -ER_k\left[\cos\left(\frac{s-\mu_k}{R_k}\right) - 1\right]\sin\ \eta_k + \Psi_E(\mu_k) & \text{if } \mu_k < s \le \lambda_{k+1},\ k = 1,\ldots,N-1. \end{cases} \tag{3}$$

A simplified potential of the ion-ion Coulombic forces contains only interactions of ions that are in the same segment or the same loop. Thus the simplified potential of the electric field acting on the nth lithium ion in the linear segment $\lambda_k \leq s_n \leq \mu_k$ is

$$\Psi_{\mathrm{Li}^+}(s,s') = \frac{1}{4\pi\varepsilon_0\varepsilon} \sum_{\lambda_k \leq s_i \leq \mu_k,\ i \neq n} \frac{q_{\mathrm{Li}^+}}{|s_n - s_i|} + \frac{1}{4\pi\varepsilon_0\varepsilon} \times \sum_{\lambda_k \leq s_i' \leq \mu_k} \frac{q_{I^-}}{\sqrt{(s_n - s_i')^2 + r_{\mathrm{CH}}^2}} + \Phi(s_n) + \Psi_E(s_n)$$

and that of the force acting on the nth iodide ion at $\lambda_k \leq s_n' \leq \mu_k$ is

$$\Psi_{I^-}(s,s') = \frac{1}{4\pi\varepsilon_0\varepsilon} \sum_{\lambda_k \leq s_i \leq \mu_k} \frac{q_{\mathrm{Li}^+}}{\sqrt{(s_n' - s_i)^2 + r_{\mathrm{CH}}^2}} + \frac{1}{4\pi\varepsilon_0\varepsilon} \sum_{\lambda_k \leq s_i' \leq \mu_k,\ i \neq n} \frac{q_{I^-}}{|s_n' - s_i'|} + \Phi(s_n') + \Psi_E(s_n').$$

The simplified potential of the electric field acting on the nth lithium ion in the loop $\mu_k \leq s_n \leq \lambda_{k+1}$ is

$$\Psi_{\mathrm{Li}^+}(s,s') = \Phi(s_n) + \Psi_E(s_n) + \frac{1}{4\pi\varepsilon_0\varepsilon} \sum_{\mu_k \leq s_i \leq \lambda_{k+1},\ i \neq n} \frac{q_{\mathrm{Li}^+}}{2R\left|\sin\left(\frac{s_n - s_i}{2R}\right)\right|} + \frac{1}{4\pi\varepsilon_0\varepsilon} \sum_{\mu_k \leq s_i' \leq \lambda_{k+1}} \frac{q_{I^-}}{\sqrt{4R^2 \sin^2\left(\frac{s_n - s_i'}{2R}\right) + r_{\mathrm{CH}}^2}}, \tag{4}$$

and that of the force acting on the nth iodide ion at $\mu_k \leq s_n' \leq \lambda_{k+1}$ is

$$\Psi_{I^-}(s,s') = \Phi(s_n') + \Psi_E(s_n') + \frac{1}{4\pi\varepsilon_0\varepsilon} \times \sum_{\mu_k \leq s_i \leq \lambda_{k+1}} \frac{q_{\mathrm{Li}^+}}{\sqrt{4R^2 \sin^2\left(\frac{s_n' - s_i}{2R}\right) + r_{\mathrm{CH}}^2}} + \frac{1}{4\pi\varepsilon_0\varepsilon} \sum_{\mu_k \leq s_i' \leq \lambda_{k+1},\ i \neq n} \frac{q_{I^-}}{2R\left|\sin\left(\frac{s_n' - s_i'}{2R}\right)\right|}. \tag{5}$$

We have assumed here that the iodide is located at the distance r_{CH} from the axis of the helix. Figure 4 indicates that the potential barrier for the passage of a lithium ion through the loop is dominated by the applied potential and not by the Coulombic potential of the permanent charges if the radius is sufficiently large. Henceforward, we disregard the Coulombic potential.

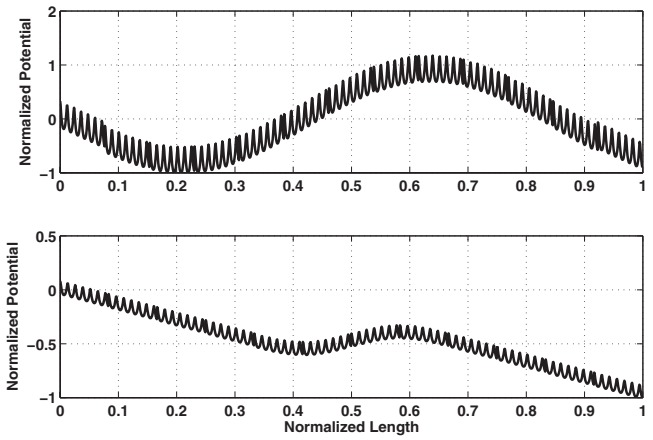

FIG. 4. The potential $\Phi(s)+\Psi_E(s)$ [Eqs. (2) and (3)] for $N=13$, $\alpha=0$, and $\eta=\pi/5$ (consisting of $N=11$ for the loop and $N=2$ for two line segments) in an unstretched (top) and for stretched (bottom) $N=13$, $\alpha=0$, and $\eta=0$ (consisting of $N=4$ for the loop and $N=9$ for two line segments). The local extrema of the potential correspond to the leftmost and rightmost points on the loop in Fig. 2.

1. Energy of one lithium and one iodide ion in the loop

According to Eqs. (4) and (5), the nondimensional potential energy of the configurations of one lithium at central angle x and one iodide ion at central angle y is

$$U(x,y) = \frac{\Phi(x,y) + \Psi_E(x,y)}{\Delta V} = -\rho\left[\cos\left(x - \frac{\pi}{2}\right) - \cos\left(y - \frac{\pi}{2}\right)\right] - \frac{10^{-6}}{\rho\sqrt{\sin^2\frac{x-y}{2} + \delta^2(x-y)^2 + \rho_{\mathrm{CH}}^2}},$$

$$0 < x < 2\pi, \quad x < y < 2\pi,$$

where the dimensionless radius of the loop is $\rho=R/L$, the constant

$$\frac{q^+}{8\pi\varepsilon_0\varepsilon\Delta V L} \approx 10^{-6},$$

is dimensionless, $\delta=d/2R$ is the dimensionless step, and $\rho_{\mathrm{CH}}=r_{\mathrm{CH}}/2R$ is the dimensionless radius of the pore. For simplicity, we keep the fixed values $\delta=0.1$ and $\rho_{\mathrm{CH}}=10^{-4}$, although they change by stretching, and investigate the energy landscape for $\rho=9\times10^{-4}$, 1×10^{-2}, 2×10^{-2}, and 3×10^{-2}. All calculations are done for $T=300$ °K and $\Delta V=3.5$ V, so that $k_BT/q^+\approx0.026$ and $q^+\Delta V/k_BT\approx134.6$.

The energy landscapes and energy contours of the configurations of a pair of lithium and iodide ions in the loop are given in Figs. 5–10 for the three chosen values of ρ. The structure of the energy landscape changes as ρ, that is, as the molecule is stretched and the radius R decreases. Figure 5 shows that for large ρ there is a potential trap for the pair, in which the ions are well separated and do not form a dipole. This configuration is created when a lithium ion enters the loop from the anode side and the iodide enters from the

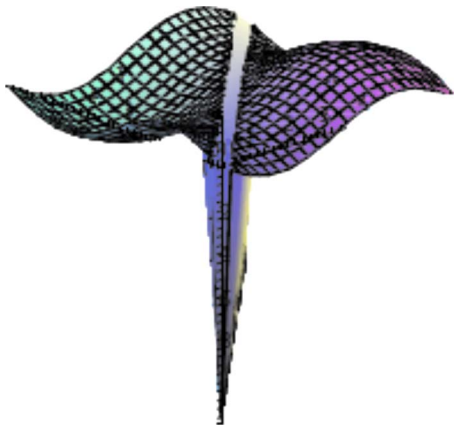

FIG. 5. (Color online) Energy landscape of the configurations of one lithium ion at central angle x and one iodide ion at central angle y in a loop of type Fig. 2 with nondimensional radius $\rho=0.03$. The energy barrier height is about $8k_BT$.

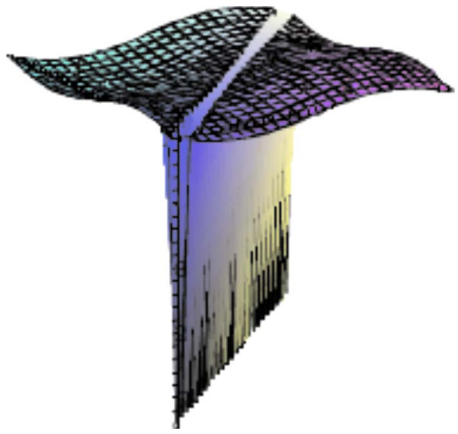

FIG. 7. (Color online) Energy landscape of one lithium and one iodide ion in the helical loop of Fig. 2 with nondimensional radius $\rho=0.02$. The energy barrier height is about $5k_BT$.

cathode side, by moving with the field. The other stable configuration is created when the ions form a dipole and diffuse together out of the loop (along the diagonal in Fig. 6), without any barrier. The two stable configurations are separated by an energy barrier given in Fig. 13.

As the effective radius of the loop is decreased to $\rho=0.02$ (Fig. 7), the barrier height drops to about $5k_BT$ and it is easier to diffuse into the other stable state, where the ions form a dipole (the diagonal in Fig. 8). Finally, as the effective radius is decreased to $\rho=0.0009$, the local minimum disappears (Fig. 9) and there is no barrier. As the two ions enter the loop, they slide down the potential slope to form a dipole (the diagonal in Fig. 10) and exit the loop by unopposed diffusion.

When there are several lithium ions in the loop, they form dipoles with the external iodide and neutralize each other. But as one lithium ion leaves into the cathode and a new one enters from the anode, the situation described above is repeated and effectively, we see only one lithium and one iodide ions that do not form a dipole as described above.

III. THE CONDUCTIVITY

The basic electrochemistry of the lithium ion battery involves only the transfer of lithium ions between the two insertion electrodes. Typical lithium ion battery consists of a carbon-based negative electrode (anode) and a lithium transition metal oxide positive electrode (cathode). Upon charging, lithium ions are extracted from the positive electrode material and inserted into the negative electrode material. Upon discharging, the reverse process is taking place. After formation of thin passivating film on the electrodes, named solid electrolyte interphase (Ref. 3) anions do not participate in the interfacial electrochemical reactions.

When a lithium ion intercalates to the cathode, the PEO is no longer electrically neutral because the iodide stays in the space between molecules. As a new lithium ion enters the loop from the anode side, an uncompensated iodide ion is drawn into the loop from the cathode side and the pair is kept apart by the external field and the other ions form dipoles. To exit the loop the separated lithium and iodide ions have to overcome the potential barrier that keeps them apart and then diffuse out of the loop as a dipole as described above. Thus the current through the loop is determined by the rate of thermal activation of the separated pair over the barrier. The rate is given by Kramers' formula,[11] generalized to two dimensions[12,13] (see Ref. 7)

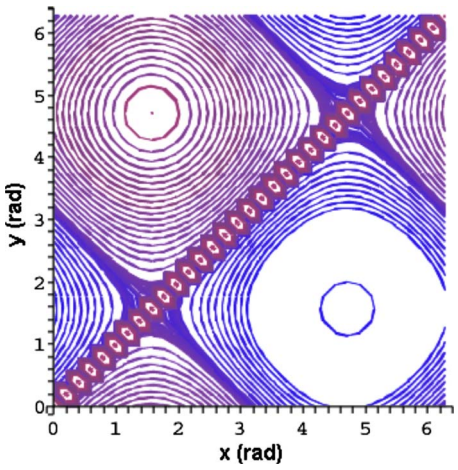

FIG. 6. (Color online) Energy contours of the landscape Fig. 5.

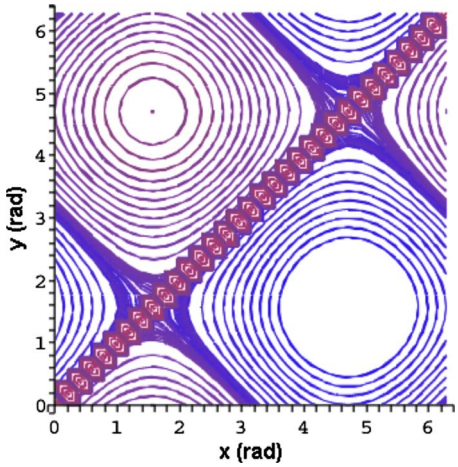

FIG. 8. (Color online) Contours of the landscape Fig. 7. Once over the barrier near the diagonal, the lithium-iodide dipole leaves the loop by free Brownian motion along the diagonal.

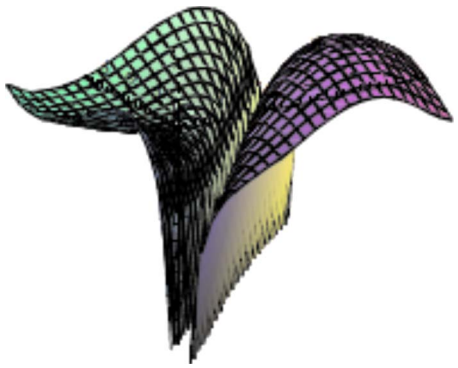

FIG. 9. (Color online) Energy landscape of a pair of lithium and iodide ions in a loop of nondimensional radius $\rho=0.0009$. There is no trap and the ions form a dipole near the diagonal.

$$\kappa = \Omega e^{-\Delta E/k_B T}, \tag{6}$$

where Ω is a steric factor that depends on the diffusion coefficient and on the geometry of the potential well. The height of the potential barrier, measured in units of $k_B T$ is given by

$$\frac{\Delta E}{k_B T} = \frac{q^+ \Delta V \Delta U}{k_B T} = 134.6 \Delta U. \tag{7}$$

The energy landscape is symmetric about the line $x+y=2\pi$ so both the minimum and the saddle point are on this line (see Figs. 11 and 12). The saddle is very flat and is weakly dependent on ρ, except for $\rho \ll 0.01$, where the barrier practically disappears, as is clearly seen in Figs. 7–10.

The barrier height is much higher for two disjoint pairs of Li^+ and I^- in the loop.

The energy barrier height is nearly a linear function of the dimensionless radius ρ for $0.01 < \rho \leq 0.03$ (Fig. 13), with a larger slope for two disjoint pairs of Li^+ and I^- in the loop.

The steric factor Ω in Eq. (6) is given by [Ref. 7, Eq. (8.6.1)]

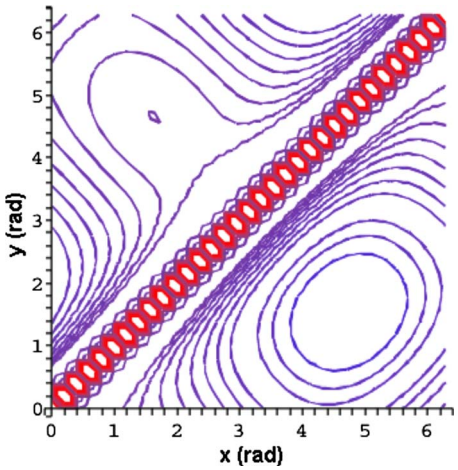

FIG. 10. (Color online) Contours of the landscape Fig. 9. The saddle point disappears when the nondimensional radius is $\rho=0.0009$.

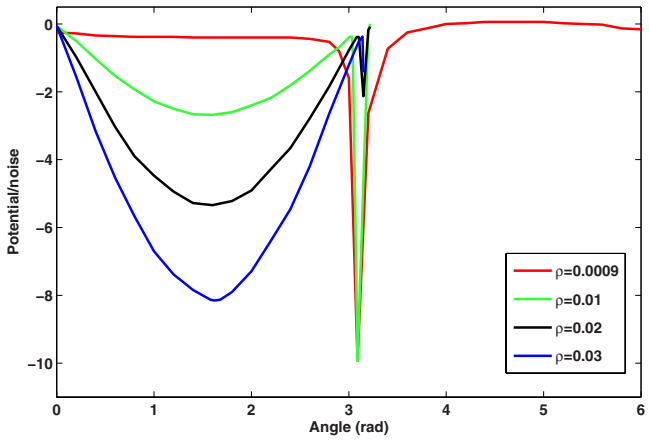

FIG. 11. (Color online) Sections of the energy surfaces of a single disjoint pair of Li^+ and I^- along the line $x+y=2\pi$. The barrier disappears at $\rho=0.0009$.

$$\Omega = \frac{\omega_1 \omega_2 \omega_4}{2\pi m \gamma \omega_3}, \tag{8}$$

where ω_1 and ω_2 are the principal frequencies of vibration at the bottom of the potential well, ω_3 is the frequency in stable direction at the saddle point, and $\omega_4 = \partial^2 U/\partial n^2|_{\text{saddle point}}$ is the frequency of imaginary vibration in the unstable direction at the saddle point. More specifically ω_1^2 and ω_2^2 are the eigenvalues of the matrix

$$\left(\begin{array}{cc} \frac{\partial^2 U(x,y)}{\partial x^2} & \frac{\partial^2 U(x,y)}{\partial x\, \partial y} \\ \frac{\partial^2 U(x,y)}{\partial x\, \partial y} & \frac{\partial^2 U(x,y)}{\partial y^2} \end{array} \right) \Bigg|_{(x,y)=\text{bottom of well}}, \tag{9}$$

and

$$\omega_3^2 = \left. \frac{\partial^2 U(x,y)}{\partial s^2} \right|_{(x,y)=\text{saddle point}}, \tag{10}$$

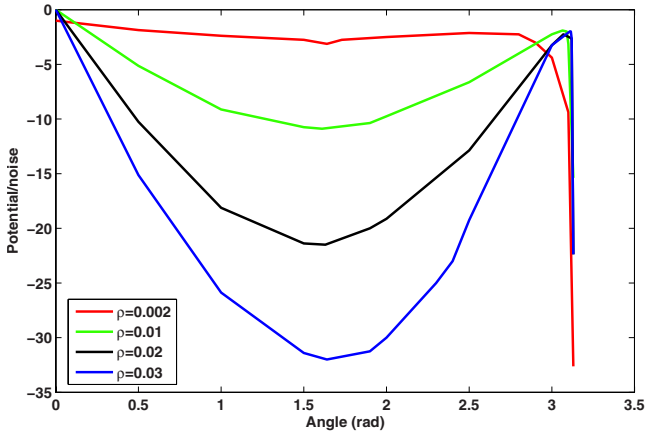

FIG. 12. (Color online) Sections of the energy surfaces of two disjoint pairs of Li^+ and I^- along the line $x+y=2\pi$. The barrier disappears at about $\rho=0.002$.

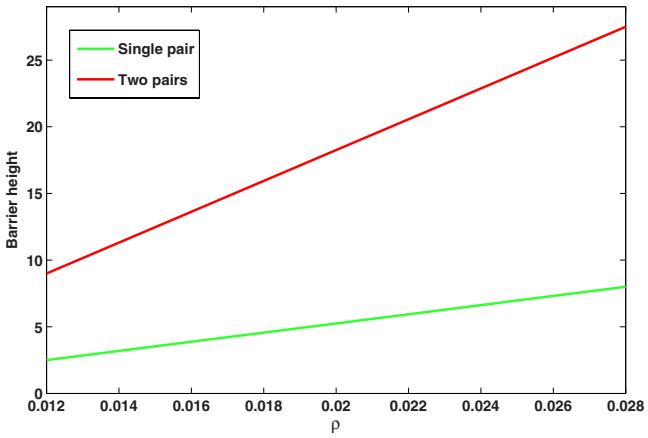

FIG. 13. (Color online) Energy barrier height in units of k_BT vs ρ.

$$\omega_4^2 = - \left. \frac{\partial^2 U(x,y)}{\partial n^2} \right|_{(x,y)=\text{saddle point}},$$

where s is arclength along the separatrix (the unstable direction) and n is the outer unit normal to the separatrix at the saddle point. The steric factor is weakly dependent on ρ, so the rate, normalized by Ω, which is the normalized current, is given by the Boltzmann factor in Eq. (6) and decays exponentially as ρ increases (Fig. 14).

Since the external voltage is fixed at about 3.5 V, the conductivity is proportional to the current with proportionality constant 3.5.

IV. DISCUSSION AND CONCLUSIONS

When the shape of a PEO molecule has some torsion, a pair of lithium and iodide ions in one winding of the molecule is kept apart by the external voltage and rests in a metastable configuration. Thermal activation of the pair over the potential barrier changes its configuration to an electrically neutral dipole, which then leaves the winded loop by unopposed diffusion. The determining factor in the process of lithium conduction in a lithium/polymer electrolyte battery is therefore the activation rate. This observation indicates that PEO conductivity is much like that in ionic crystals and is therefore given by the Nernst–Einstein type formula (6).[14] A detailed derivation of this formula is given in (Ref. 7, Chapter 8).

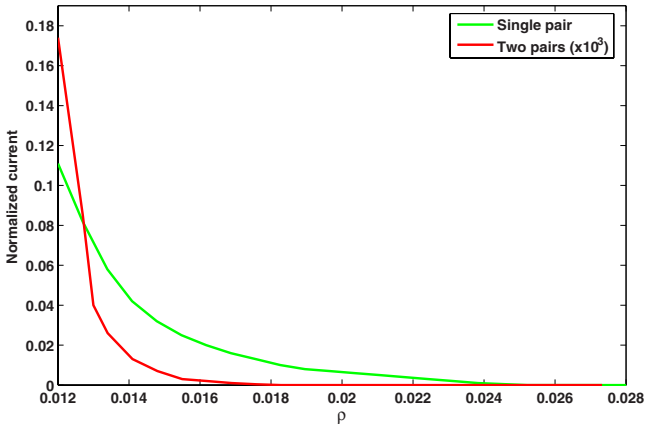

FIG. 14. (Color online) Normalized current vs ρ. The normalized current with two disjoint pairs in the loop is magnified by 10^3.

The calculation of the potential barrier and current for a loop with two disjoint pairs of Li^+ and I^- in the loop are analogous to those for a single pair as detailed above. The slope of the potential barrier height versus ρ is higher for two disjoint pairs in the loop. This indicates that stretching is more effective at higher concentrations.

The analysis of this scenario can explain the dramatic changes in conductivity observed in the simulations of Ref. 2. The exponential dependence of the activation rate on the loop radius can lead to the 40-fold increase in conductivity of the stretched polymer.

A. Experimental results

Machine stretching of the polymer electrolyte films with different concentration of LiI salt in PEO matrix has been carried out at room temperature at constant rate of 10.6 mm/min.

The ionic conductivity of polymer electrolyte in the longitudinal direction has been measured *in situ*. During stretching the length of the film increases. This is followed by alignment of the helixes of the polymer chains and favors the ionic transport of lithium cation inside the helices. In addition, longitudinal orientation of helices promotes the cation jump from helix to helix.

On stretching, the conductivity orthogonal to film plane decreases, that once again showed that stretching orders the structure of LiI:P(EO)n polymer electrolytes. The higher is the speed of stretching, the lower is the conductivity enhancement.

B. Numerical results

We capture in our model this stretching-induced onset of order by representing the main geometrical features of the polymer molecule in terms of randomly oriented linear segments and circular loops and their transformation by stretching (see Fig. 1). Linear segments tend to align in the direction of stretching and the radii of circular loops decrease. The effect of conformational changes on conductivity is captured in our simplified model of Li^+/I^- motion. The percentage of stretching corresponds to change changes in ρ in our model from 0.16 down to 0.0001.

The simulation results show good agreement with experimental data of the effect of stretching on the longitudinal conductivity of LiI:$P(EO)_{20}$, LiI:$P(EO)_7$, and LiI:$P(EO)_9$ at room temperature (Figs. 15 and 16). The agreement is not only in the correct trend (increase in the conductivity with stretching, slope of the graph) but also in the absolute values of the conductivity. While the simulations accounts for the qualitative observations, the good agreement with experimental data supports the validity of our model.

In Fig. 15, relevant to this concentration, the curves corresponding to smaller salt concentration are presented also, for LiI:$P(EO)_{40}$ and LiI:$P(EO)_{100}$. There are no experimental data relevant to this concentrations.

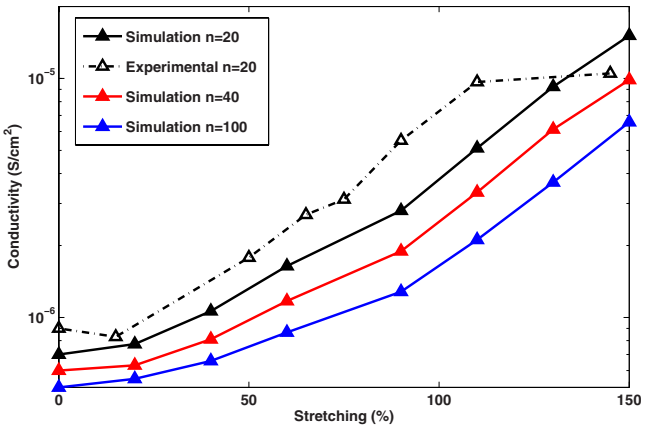

FIG. 15. (Color online) Simulation conductivity (S/cm^2) vs stretching at concentration ratios LiI:P(EO)$_{20}$ at room temperature.

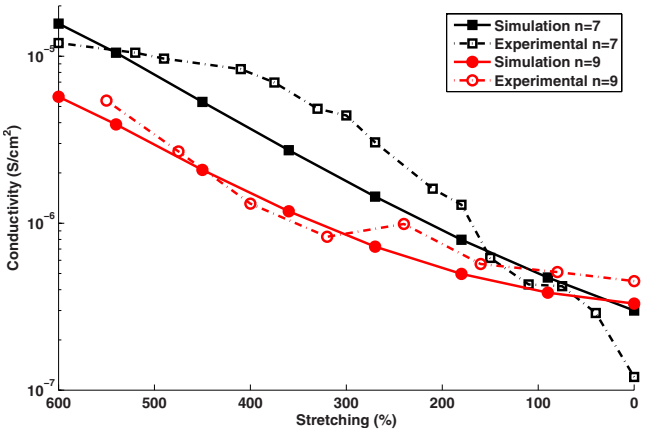

FIG. 17. (Color online) Experimental and Simulation conductivity (S/cm^2) vs stretching at concentration ratios LiI:P(EO)$_7$ at room temperature.

The experimental and numerical data collected on Fig. 15, correspond to concentrations from $n=20$ to 100. The conductivity enhancement (slope of the graph) is higher in the more concentrated polymer electrolyte. This indicates that stretching is more effective at higher concentrations, which is explained by the fact that the slope of the potential barrier height versus ρ is higher for two disjoint pairs in the loop, as shown in the Fig. 13. Figure 16 shows similar results for LiI:P(EO)$_7$ and LiI:P(EO)$_9$. However, due to the peculiarities of the structure of these polymers, they have to be studied separately. For LiI:P(EO)$_n$, $n=20/100$, the PEO chains adopt helical conformations with all C–O bonds trans and C–C bonds either gauche or gauche minus. Each PEO chain is associated with a dedicated set of cations and anions that do not coordinate to any other chain. In other words, there is no ionic cross-linking between chains, only weak van der Waals interactions.

Increasing the polymer:salt ratio from 3:1 to 6:1 has a profound influence on the crystal structure (see Ref. 5). The cations are arranged in rows with each row being located within a cylindrical tunnel formed by two PEO chains. The chains are not helical. Each chain forms the surface of a half-cylinder and the two chains interlock on each side to complete the cylindrical arrangement. The anions do not coordinate the cations but are instead located outside the dimensions of the PEO cylinder in the interchain space.

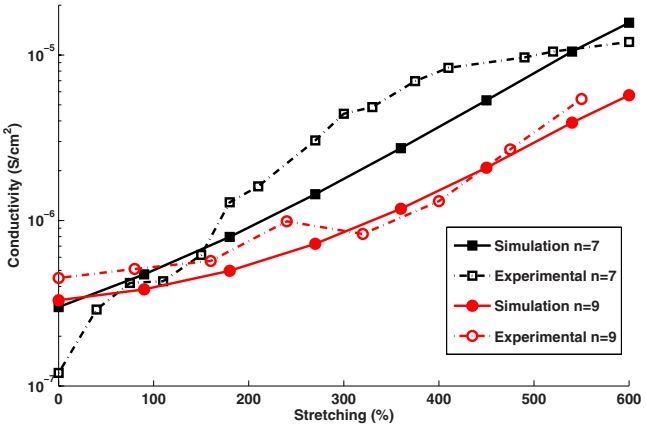

FIG. 16. (Color online) Simulation conductivity (S/cm^2) vs stretching at concentration ratios LiI:P(EO)$_7$ at room temperature.

The stretched LiI:P(EO)$_7$ polymer electrolyte has highly elastic rubber structure, the relaxation of which in the process of stretching starts immediately after release of the load. To achieve nonreversible structural changes the film of LiI:P(EO)$_7$ electrolyte was kept under the load at about 65 °C for at least 12 h. The LiI:P(EO)$_9$ polymer electrolyte behaves similarly on stretching; its rubber properties, however, are less pronounced. Dilute polymer electrolyte LiI:P(EO)$_{20}$ was only partially stretched because its structure does not allow further stretching.

In our simplified model, we assume that the stretched polymer adopts a modified helical structure, similar to that of an extended salt-free PEO helix but no cylindrical tunnel is formed by two PEO chains. Everything else is in line with experimental data. In this conformation, all the CH_2 groups face outward. This facilitates wagging and twisting out-of-plane deformations. In the aligned conformation of the helix the oxygen atoms are directed inward, lining the tunnel cavity, thus favoring cation transport. Despite its simplicity, our model indicates that LiI:P(EO)$_7$ has the maximum conductivity enhancement in the stretch, as seen from experimental data. This is attributed to highly aligned cylindrical tunnels for Li^+ transport in double PEO chains coordinating the cations, as suggested by[5] and tends to support the validity of our model.

If the cation/polymer substructure is maintained, then in both the 3:1 and 6:1 compositions the cations remain within tunnels defined by the PEO chains. If this is the case, then a random arrangement of chains, such as might be envisaged in a simple amorphous polymer, is not conducive to ion transport. Instead, by organizing chains in a more aligned fashion, transport along and between chains is facilitated.

The steric factor is weakly dependent on ρ, i.e., on the percentage of stretching, so the rate, which is the conductivity, is given by the Boltzmann factor in 3.1) and thus decays exponentially as ρ increases (see Fig. 14 for a single and two pairs). Figures 17 and 18 show the same for different concentrations.

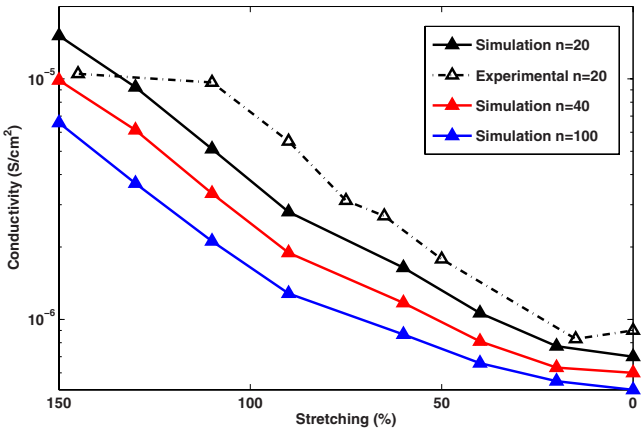

FIG. 18. (Color online) Experimental and Simulation conductivity (S/cm^2) vs stretching at concentration ratios $LiI:P(EO)_{20}$, $LiI:P(EO)_{40}$, and $LiI:P(EO)_{100}$ at room temperature.

We believe that theoretical insight into the transport processes can help in research and development of new rigid polymers with ordered channels and composition for enhanced ion transport.

ACKNOWLEDGMENTS

The first three authors were supported by a Grant No. 2004403 from the U.S.-Israel Binational Science Foundation. The research of Z. Schuss was partially supported by a research grant from TAU. Thanks for Dr. Ela Lifshits for providing the experimental data from her Ph.D. studies under the supervision of Professor E. Peled and Professor D. Golodnitsky, School of Chemistry, Tel Aviv University.

[1]L. Gitelman, M. Israeli, A. Averbuch, M. Nathan, Z. Schuss, and D. Golodnitsky, J. Comput. Phys. **227**, 1162 (2007).
[2]L. Gitelman, M. Israeli, A. Averbuch, M. Nathan, Z. Schuss, and D. Golodnitsky, J. Comput. Phys. **227**, 8437 (2008).
[3]E. Peled and D. Golodnitsky, in *Solid-Electrolyte Interphase*, edited by P. Balbuena and Y. Wang (Imperial College Press, World Scientific, London, 2004), pp. 1–70.
[4]M. B. Armand, Annu. Rev. Mater. Sci. **16**, 245 (1986).
[5]Y. G. Andreev and P. G. Bruce, Electrochim. Acta **45**, 1417 (2000).
[6]B. Hille, *Ionic Channels of Excitable Membranes* (Sinauer Associates, New York, 1993).
[7]Z. Schuss, *Theory and Applications of Stochastic* (Wiley, New York, 1980).
[8]A. Aabloo and J. Thomas, Solid State Ionics **143**, 83 (2001).
[9]B. A. Ferreira, A. T. Bernardes, and W. B. De Almeida, J. Mol. Struct.: THEOCHEM **539**, 93 (2001).
[10]H. Tadokoro, J. Polym. Sci. C **1**, 119 (1967).
[11]H. Kramers, Physica (Utrecht) **7**, 284 (1940).
[12]H. C. Brinkman, Physica (Utrecht) **22**, 149 (1956).
[13]J. S. Langer, Ann. Phys. (N.Y.) **54**, 258 (1969).
[14]L. Girifalco, *Atomic Migration in Crystals* (Blaisdell, Waltham, Mass., 1964).